Antifouling graphene oxide-polyvinylidene fluoride mixed matrix membrane for membranes distillation applications

Enrica Fontananova[a,*], Valentina Grosso[a], Andreas A. Sapalidis[b], Elena Tocci[a], Gianluca Di Profio[a]

[a]Institute on Membrane Technology of the National Research Council (ITM-CNR), Via P. Bucci, cubo 17/C,
at University of Calabria, 87036 Rende (CS), Italy, Tel. +39 0984492010; email: e.fontananova@itm.cnr.it (E. Fontananova)
[b]Institute of Nanoscience and Nanotechnology, National Center for Scientific Research "Demokritos",
Terma Patriarxou Grigoriou kai Neapoleos, Agia Paraskevi Attikis, 153 41, Athens, Greece

ABSTRACT

Porous hydrophobic mixed matrix membranes with antifouling properties were produced by synergic combination of graphene oxide (GO) with polyvinylidene fluoride (PVDF). The protocol developed was easily scalable and environmentally friendly. This last property was guaranteed by the use of a not-toxic solvent (dimethyl sulfoxide) to solubilize the polymer and properly disperse the GO, a green non-solvent (water) to induce phase separation and the absence of any pore forming additive in the casting solution. The presence of the 2D-nanofiller in the casting solution influenced surface charge but also the structure of the formed membranes inducing the formation of crystallites (prevalently in the β-form) with larger dimensions with respect to the polymeric PVDF prepared without GO. Membrane fouling caused severe declining of flux in PVDF membrane in direct contact membrane distillation (DCMD), as a result of the relevant deposition of humic acids on the hydrophobic surface of the membrane. On the contrary, mixed matrix PVDF-GO was less prone to fouling, as confirmed by surface characterization techniques and stable performance in DCMD before and after prolonged contact with humic acids.

Keywords: Crystallites; Fouling; Graphene oxide; Membrane distillation; Phase separation; Polyvinylidene fluoride; Zeta potential

1. Introduction

Global water demand is projected to increase by 55% between 2000 and 2050 [1] as a consequence of the population increase, the intensive development of the industrial, agricultural and energy sectors, as well as, the negative impact of climate changes on world water resources. This continuously growing water demand is imposing a further technological development in water desalination and wastewater treatment. Membrane technology offers several sustainable and cost-effective opportunities of turning saline or contaminated water into drinking water. In this perspective membrane distillation (MD) represents an innovative membrane operation able to use low-grade or waste heat, such as geothermal and waste heat from power plants and industrial facilities. Moreover, the use of renewable energy sources like solar is able to improve the water-energy nexus [2–4]. A relevant advantage of MD in comparison to traditional thermal processes such as multi-effect distillation and multi-stage flash distillation, is the relatively small areal footprint thanks to the modular membrane system configuration, particularly advantageous for small scale and portable systems. With respect to other membrane processes like reverse osmosis (RO)

process, MD can operate at higher feed concentration. In a MD process a porous hydrophobic membrane is used as a non-selective interface placed between an aqueous heated solution on the one hand (feed or retentate) and a condensing phase (permeate or distillate) on the other. The hydrophobic nature of the membrane, generally polymeric, prevents penetration of the pores by aqueous solutions due to surface tensions and allows the establishment of a vapor–liquid interface at the entrance of each pore. The temperature gradient between the two streams leads to a vapour pressure difference causing volatile compounds (commonly water) evaporation on the hot feed solution-membrane interface, transfer of the vapour phase through the membrane pores, and condensation on the cold side membrane-permeate solution interface. High hydrophobicity, low fouling tendency, narrow pore size distribution, elevated porosity, excellent chemical resistance, long-term stability, low thermal conductivity and suitable thickness, represent target membrane's properties for efficient MD processes [5]. Currently, hydrophobic micro- and ultra-filtration membranes, are often used in MD applications. However, these membranes don't completely satisfy the specific demands of this process. Fouling, scaling, and wetting still have a significant detrimental impact on MD performance [4]. Another challenge that membrane manufacturing industry and academic world are facing in recent years, is the necessity to develop sustainable membrane preparation protocols avoiding the use of substances of very high concern like N,N-dimethylacetamide (DMA), N,N-dimethylformamide (DMF), and 1-methyl-2-pyrrolidone, widely used as solvents for the production of several polymeric membranes [6–8]. The development of porous hydrophobic membranes specifically designed for MD and produced at acceptable costs via sustainable protocols, it is of paramount importance to improve the application in industrially relevant environment of this promising membrane operation. In the last years nanotechnology has opened new opportunities for researching new membrane materials, or modifications of existing ones. Nanostructured materials such as zeolites, metal organic frameworks and carbon based, have attracted considerable attention as alternative membrane materials or functional additive in mixed matrix membranes to replace polymeric membranes due to their good chemical resistance, high flux, and specific transport properties [9]. Graphene-based membranes are promising candidates for aqueous separations. Fast water permeation routes that can be achieved in stacked graphene sheets by the low-friction flow of a monolayer of water, but also combined size and electrostatic ion exclusion mechanisms through 2D nanocapillaries of graphene derivative such as graphene oxide (GO) [10–14].

In this work, GO was used as functional additive in polyvinylidene fluoride (PVDF) membranes. Previous literature works reported the use of GO in combination with PVDF [15–17]; however, the membranes were prepared using toxic solvent like DMA [15] and DMF [16,17]. Moreover, the membranes were characterized by low water contact angles that render these systems not applicable for membrane contactor applications.

In the present study, porous membranes with high surface roughness and hydrophobicity were prepared by an environmentally friendly method by using non-toxic solvents in a combined vapour- and liquid-induced phase separation method (VIPS and LIPS, respectively) without chemical pore forming additives. The presence of the GO conferred antifouling properties to the mixed matrix membranes as confirmed by the lower absorption of humid acids on the membrane surface, while maintaining high flux and rejection in membrane distillation applications.

2. Materials and methods

GO powder (particle size: D90 25–28 μm, D50 13–15 μm; D10 6–7 μm) was purchased from Graphenea. PVDF Solef 6010 was kindly supplied by Solvay Solexis. Dimethyl sulfoxide (DMSO), sodium chloride (NaCl) and humic acid (HAs, technical grade) were purchased from Merck. RO water was used for solution preparation and as coagulation bath in LIPS (Zeneer RO 180 water purification system).

2.1. Membranes preparation

The GO was dispersed in DMSO by sonication using a digital ultrasonic bath ArgoLab DU-32 (ultrasonic power 120 W, frequency 40 kHz, sonication time 30 min). The PVDF was gradually added to the GO-DMSO dispersion and solubilized under magnetic stirred at 60°C for 48 h (polymer concentration 18 wt.%). The final loading of GO in the formed PVDF-GO membrane (i.e., after solvent removal) was 1 wt.% with respect to polymer. Moreover, a PVDF polymeric membrane was also prepared as reference sample in the same experimental conditions but without GO. Water was used as green non-solvent in a combined VIPS and LIPS process [7]. The PVDF or PVDF-GO solution was cast with an initial thickness of 200 μm onto a non-woven fabric by an automatic casting machine (TQC AB3120; casting rate 2 mm/s). The cast film was exposed for 5 min to an atmosphere with relative humidity 50% ± 2% and temperature 30°C ± 1°C in order to have an initial phase separation by VIPS process. The polymer precipitation was completed by immersing the cast film in a water coagulation bath to induce the LIPS process. The formed membranes were washed with water and then dried at 25°C for an additional day. The membranes were stored in a dry state until the use.

2.2. Membrane characterization and testing

The membranes' upper surface and cross section were observed by an EVO MA10 Zeiss scanning electron microscope (SEM). Surface roughness was measured by a Nanoscope III atomic force microscope (AFM) (Digital Instruments, VEECO Metrology Group) in air, in contact mode imaging. Roughness data were elaborated by WSxM 5.0 Develop 6.1 software (Nanotec Electronica S. L) to measure the root mean square roughness (RMS). Water contact angle (CA) measurements were carried out using a CAM 200 device (KSV Instruments, Ltd.). The mean pore diameter of the membranes was measured by a capillary flow porometer (PMI, Porous Materials Inc. Ithaca, NY) using as wetting liquid 3MFluorinert™ Electronic Liquid FC-40 (Essegie Srl) and nitrogen as pressurising gas. The membrane total

porosity was measured by gravimetric method with the same type of wetting liquid used for the capillary flow porometry. The liquid entry pressure of water (LEP) was experimentally terminated measuring the pressure difference at which liquid water penetrates into the membrane's pores using nitrogen as pressuring liquid in a dead-end cell (4.7 cm diameter) at room temperature. Electrokinetic analyses were carried out by Surpass™ 3 (Anton Paar) analyzer using streaming potential and streaming current method for a direct analysis of the membrane surface zeta potential. The solution used was 5 mmol/L KCl aqueous solution in the pH range of 2–9.

Fourier-transform infrared spectroscopy (FTIR) analyses in attenuated total reflectance (ATR) were performed using a Perkin Elmer Spectrum One (Perkin-Elmer) to quantify the β-phase content of the crystalline portion of the PVDF [18,19].

The membrane transport properties were tested in direct contact membrane distillation (DCMD) [20]. Performances were evaluated in terms of water flux and rejection using 0.5 M NaCl as feed and RO water as distillate side solution. Operating conditions were: feed and distillate temperature 50°C ± 1°C and 20°C ± 1°C, respectively; feed and distillate solutions flow rate 12 L h^{-1} (axial velocity 6.1 m h^{-1}); membrane active area 2.4×10^{-3} m^2.

Each test lasted 6 h and the flux and rejection were taken as the average value under steady conditions (normally after the first 2 h of operation and until the end of the test).

Fouling test was carried out by immersing a membrane sample for 48 h in a solution composed of NaCl 0.5 M and 0.1 g/L of humic acids and then immersed in clean water for 48 h to remove weakly adsorbed substances. Finally, the membrane was tested again in DCMD test and characterized by SEM and FTIR analyses, as reported above.

3. Results and discussion

DMSO was selected as water-miscible, non-hazardous, high-boiling, biodegradable, and recyclable solvent [8] to solubilize PVDF. DMSO was also able to well disperse the GO nanoflakes thanks to its high dipole moment (3.96 D). The dispersion of the GO was further improved by sonication procedure. Water was used as green non-solvent both, in vapour and liquid phases during the combined VIPS-LIPS process. The mixed matrix PVDF-GO membranes was characterized by a uniform grey colour vs. the white colour of the polymeric membrane (Fig. 1). The homogeneity of the grey coloration was a first qualitative indication of a good dispersion of the GO in the PVDF matrix.

The prepared membranes showed a porous surface characterized by spherulitic microparticles linked together through fiber-like connections and characterized by surface micro-protrusions responsible of the high surface roughness of the membranes (Fig. 2a and b). The use the non-woven fabric as support, visible in the bottom part of the membrane cross section (Fig. 2c and d), improves the mechanical properties of the sample with respect to unsupported membranes (tensile strength >25 MPa in the presence of the support [21]). However, the support did not limit the permeation rate through the membrane thanks to its elevated porosity which also allows the penetration of the polymeric solution during the casting process. Moreover, it also favours the potential upscaling of the protocol in roll-to-roll industrial casting systems [7].

The slow diffusion of the non-solvent from vapor phase into the cast solution (VIPS stage) induced locally microphase separation on the membrane surface with the formation of nucleation clusters of polymer crystallites [7,21]. As a consequence, the phase separation process is characterized by a quite uniform concentration profile of the three components: precipitant, polymer and solvent. This induced the shaping of a membrane with a more porous and rougher surface with respect to a membrane prepared by direct immersion in liquid water (i.e., by LIPS) [7,21]. The membrane formation process was completed by the immersion in the liquid coagulation bath (LIPS stage). The PVDF crystallites were prevalent in the b-phase, the thermodynamically stable form of the PVDF, as confirmed by the analyses of the ATR-FTIR spectra showing characteristic signals of α (763, 795, 854, 975, and 1,384 cm^{-1}) and β polymorphs (840, 1,172 and 1,273 cm^{-1}) [18,19,22], with a dominance of the second one: 84.5% ± 0.1% and 86.2% ± 0.1% of β-phase for the polymeric and mixed matrix membranes, respectively. The slightly higher content of the b-phase in the PVDF-GO membrane can be explained
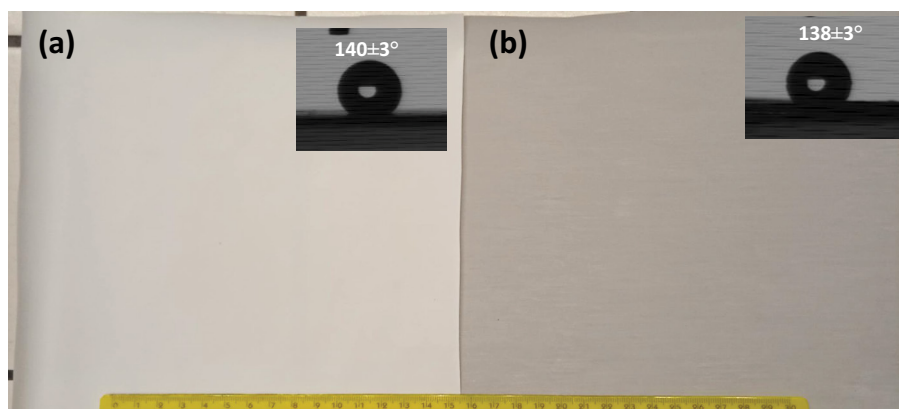

Fig. 1. Image of the polymeric PVDF (a) and the mixed matrix PVDF-GO membrane (b). In the insert is reported the profile of a water drop on the membrane surface taken during contact angle measurements and the corresponding medium value.
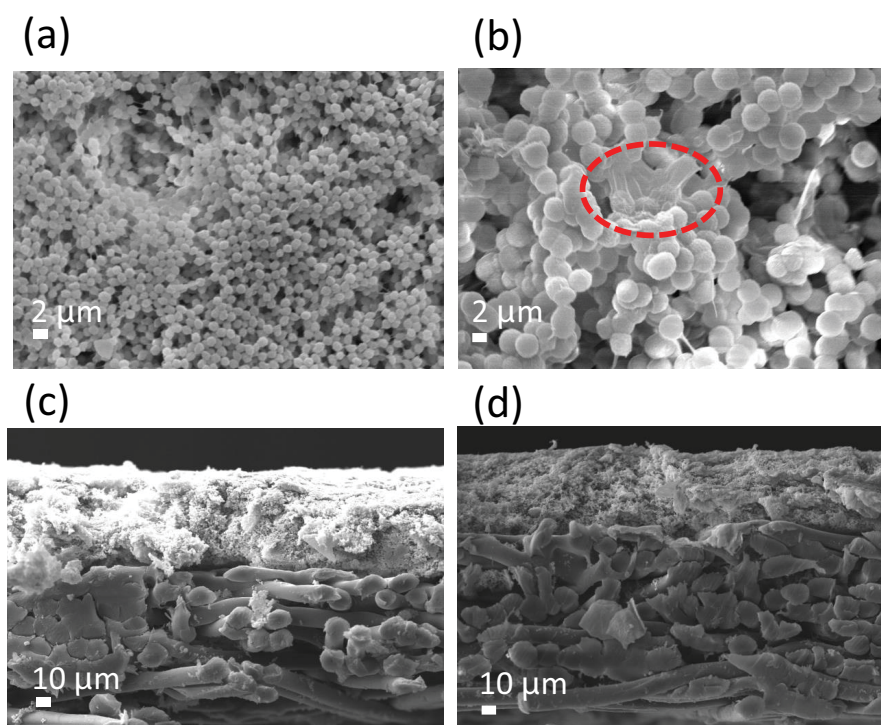
Fig. 2. (a) SEM images of the surface of the PVDF polymeric and (b) PVDF-GO mixed matrix membrane and the corresponding cross-section ((c, d), respectively). The red oval in (b) highlights a GO flake embedded in the PVDF matrix.

by considering the presence of the polar groups on GO in addition to the use of a polar solvent (i.e., DMSO).

The high surface roughness of the PVDF membrane, combined with the hydrophobic nature of the polymer determined the high-water contact angle (Fig. 1) and the consequent high-water liquid entry pressure (Table 1). These value are higher than those reported in previous works in which the GO was used as functional additive in PVDF membranes prepared by phase separation methods but without a VIPS stage [15,16].

The mixed matrix membrane was characterized by lamellar nanostructures embedded into the PVDF that can be attributes to the GO nanoplates (Fig. 2b). Micro Raman spectroscopy confirmed that the lamellar structures observed in the SEM images of the mixed matrix membrane corresponded to GO. The Raman spectra of the black spots individuated by optical microscope integrated in the Raman instrument showed the typical D-, G- and 2D-bands at 1,348, 1,590 and 2,700 cm^{-1}, respectively (Fig. 3). The low intensity of the 2D band indicate a multilayers structures of the GO embedded in the PVDF matrix.

PVDF crystallites were formed also in the neat membrane, however the dimensions of the spherulities in the mixed matrix membrane were higher in comparison with the polymeric membrane (Fig. 2a and b). This effect was due to a delayed liquid–solid demixing mechanism induced by the GO presence which increased the solution viscosity, favoring crystallite growth before membrane solidification (kinetic effect on the phase separation process [23]). Moreover, the presence of the GO in the membrane, did not induce any detrimental impact on the
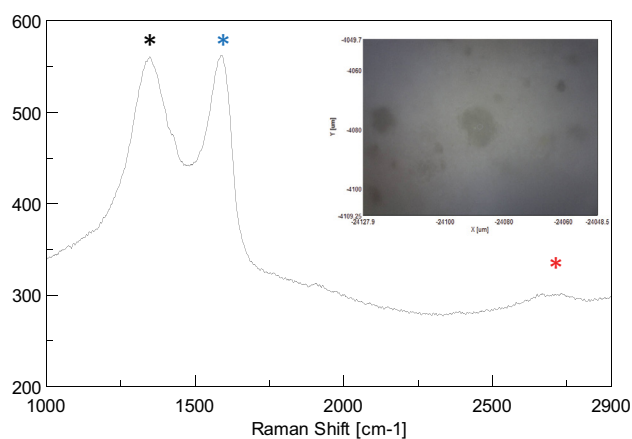

Fig. 3. Raman spectra of the PVDF-GO mixed matrix membrane. The black, blue and red stars indicate the position of the D-, G- and 2D-band, respectively. The insert reports the image of the membrane surface taken by an optical microscope integrated in Raman spectrophotometer.

wetting resistance of the PVDF-GO membrane. Despite the lower surface roughness of the PVDF-GO membrane (Table 1 and Fig. 4), the mixed matrix membrane was also characterized by a high hydrophobicity and LEP (Table 2), making it ideal for MD applications.

The PVDF and PVDF-GO were tested in DCMD test using as feed NaCl 0.5 M as seawater model solution and

Table 1
Properties of the PVDF polymeric and PVDF-GO mixed matrix membrane

Membrane	PVDF	PVDF-GO
RMS (µm)	0.83 ± 0.08	0.53 ± 0.07
Mean pore size (µm)	0.20 ± 0.02	0.22 ± 0.02
Total porosity (%)	73 ± 2	75 ± 3
Liquid entry pressure (bar)	2.0 ± 0.2	1.8 ± 0.2
Thickness (µm)	153 ± 4	160 ± 5

a thermal gradient compatible with the conditions achievable by solar assisted systems. The results evidenced almost similar transmembrane flux for both, polymeric and mixed matrix membranes (Table 2), as expected considering the similar mean pore size, thickness and total porosity of the membranes (Table 1).

However, the presence of the GO increased membrane rejection due to its influence on membrane microstructure, combined with electrostatic and barrier effects of the GO lamellae. The performance of this membrane did not change in relevant way after prolonged contact with saline solution (>30 days).

As already stated, MD process faces the challenge of fouling caused not only by inorganic salts scaling but also by organic fouling due to natural organic matter (NOM) present in natural water sources [24]. It has been reported that humic substances are the major NOM components present in natural water sources such as seawater [25]. In order to study the fouling tendency of the membranes

prepared, they were immersed in a solution composed by NaCl and HAs (Fig. 5a). It is important to note that the amount of HA sused was about 286 times higher than those occurring in natural seawater (about 0.35 mg/L of HAs in seawater [26]) in order to accelerate and maximize organic fouling phenomena.

Fouling layer deposited on the PVDF polymeric membrane (Fig. 5b) imposed an additional resistance to mass transfer. The fouled PVDF membrane showed a relevant reduction of the flux with respect to unfouled sample and decline of the water contact angle (–64% and –26%, respectively; Table 2). This effect was due to the strong absorption of the organic matter on the polymeric hydrophobic membrane with consequent increase of the mass transport resistance and decrease of the membrane hydrophobicity. No detrimental impact of the fouling on the membrane rejection was observed (+1.4%; Table 2). The fouling by HAs was also confirmed by ATR-FTIR analyses carried out on the pristine and fouled membranes. Characteristic signals of HAs were in fact observed on the surface of the fouled PVDF polymeric membrane: O–H stretching at 3,600–3,000 cm^{-1}; C=O and C=C stretching at 1,750–1,500 cm^{-1} (Fig. 5d).

On the contrary, the membrane containing GO showed only a moderate reduction of the flux and water contact angle (–10% and –18%, respectively; Tab. 3). The presence of the GO in the PVDF membrane reduced the fouling tendency thanks to the specific properties of this 2D-nanomaterial characterized by a low interacting graphitic structure combined with the presence of hydrophilic oxygenated groups, which reduced the absorption of organic substances onto hydrophobic PVDF surface (Fig. 5c and e). Moreover, the presence of PVDF crystallites with higher dimensions
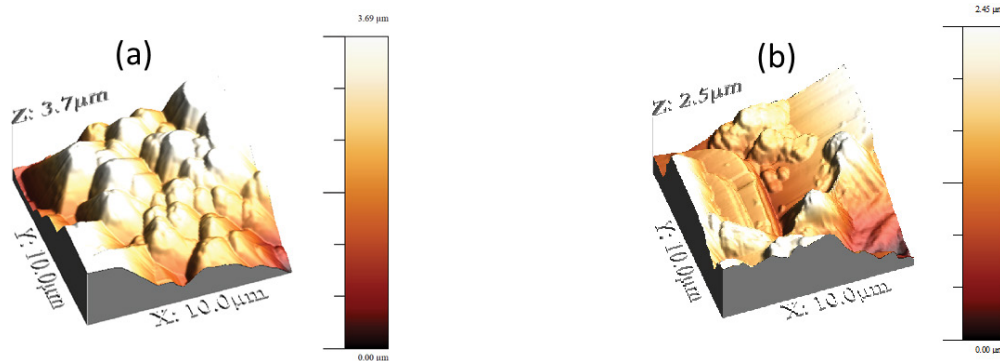

Fig. 4. 3D AFM height images of the surface of: (a) the PVDF polymeric and (b–c) the PVDF-GO mixed matrix membrane.

Table 2
Flux and rejection of the PVDF polymeric and mixed matrix PVDF-GO before and after fouling

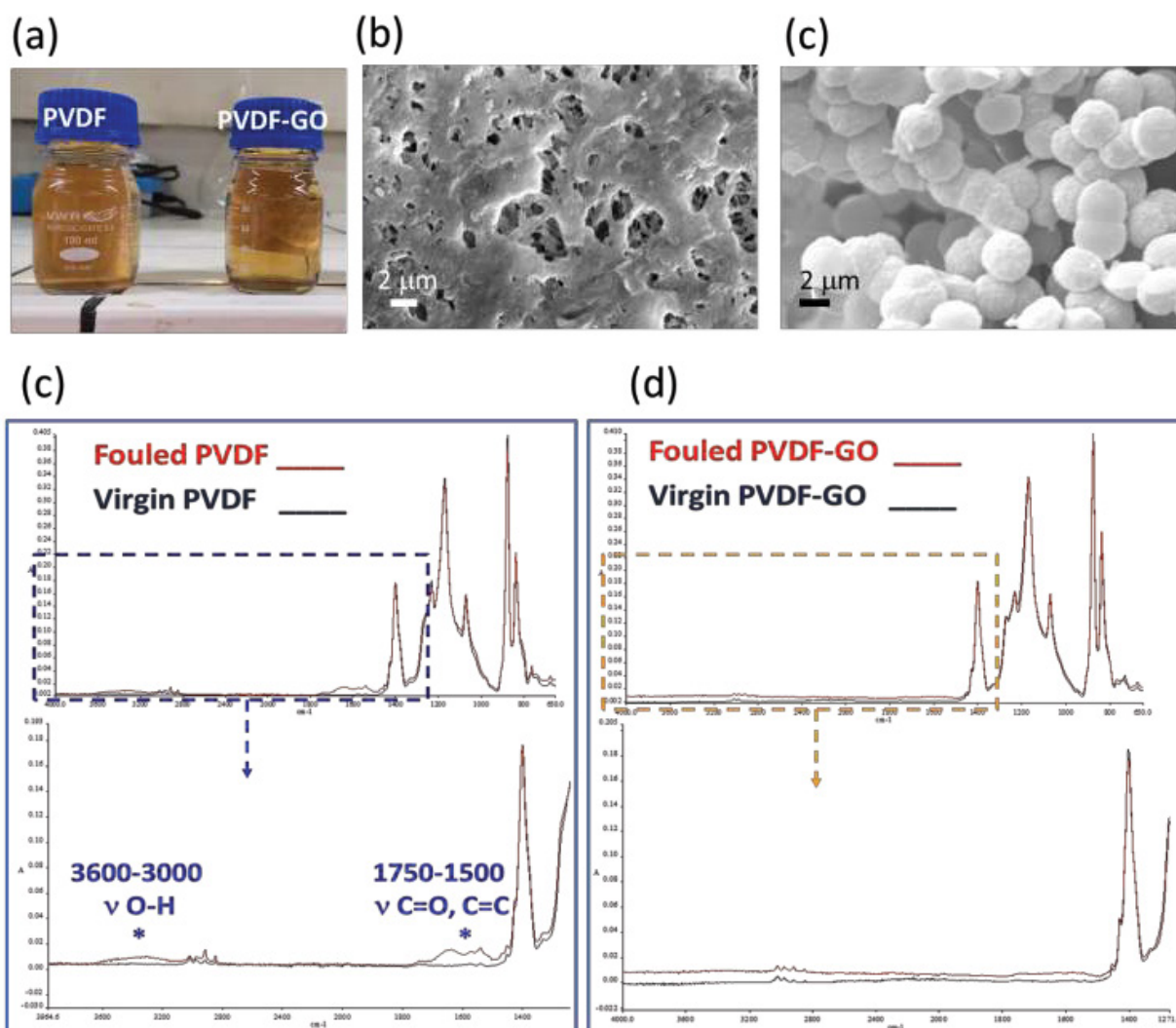| Membrane	Property	Pristine membrane	Fouled membrane
PVDF	Contact angle (°)	140 ± 3	104 ± 3
	Flux (kg h^{-1} m^{-2})	11 ± 2	4 ± 1
	Rejection (%)	95.7 ± 0.1	97.0 ± 0.1
PVDF-GO	Contact angle (°)	138 ± 3	113 ± 3
	Flux (kg h^{-1} m^{-2})	10 ± 1	9 ± 1
	Rejection (%)	99.99 ± 0.01	99.99 ± 0.01

Fig. 5. Image of the PVDF and PVDF-GO samples immersed in NaCl-humic acids solution during the fouling test (a); SEM image of the surface of the PVDF (b) and PVDF-GO (c) after fouling; ATR-FTIR spectra of the PVDF (d) and PVDF-GO (e) pristine (black line) and fouled (red line) samples.

in the case of the PVDF-GO with respect to the PVDF membrane (Fig. 2a and b), is also expected to reduce the absorption phenomena thanks to a reduced surface area.

The zeta potential is related to the surface charge at a membrane/liquid interface and it is a key parameter for understanding membrane surface properties, including fouling tendency [27]. The pristine PVDF-GO membrane has an isoelectric point (IEP) higher than the PVDF membrane (3.9 vs. 3.7 mV, respectively) and slightly less negative zeta potential at pH > IEP (Fig. 6a), as a consequence of the presence of acid groups on the GO (mainly carboxylic and phenolic groups). The polymeric PVDF membrane after contact with HAs showed a more relevant decrease of the IEP with respect the mixed matrix membrane (3.4 vs. 3.7 mV, respectively; Fig. 6b and c). This effect was due to the strong absorption of HAs (mainly in sodium form [28]) forming a layer on the polymer membrane surface (Fig. 5b), which reduced the absolute value of the

zeta potential at pH > 5, contributing to a further accumulation of organic matter on the polymeric membrane surface.

4. Conclusions

The results obtained validated a sustainable and scalable way to produce hydrophobic PVDF-GO composite membranes, suitable for membrane distillation applications. In the developed protocol, DMSO was selected as non-hazardous solvent, in place of traditional substances of very high concern, in a combined vapour- and liquid-induced phase separation process, using water as non-solvent, and without the use of any chemical additive as pore former. The membranes were characterized by a spherulitic morphology with high surface roughness. The PVDF-GO membrane showed improved rejection and similar flux in comparison with a polymeric sample prepared by the same protocol but without
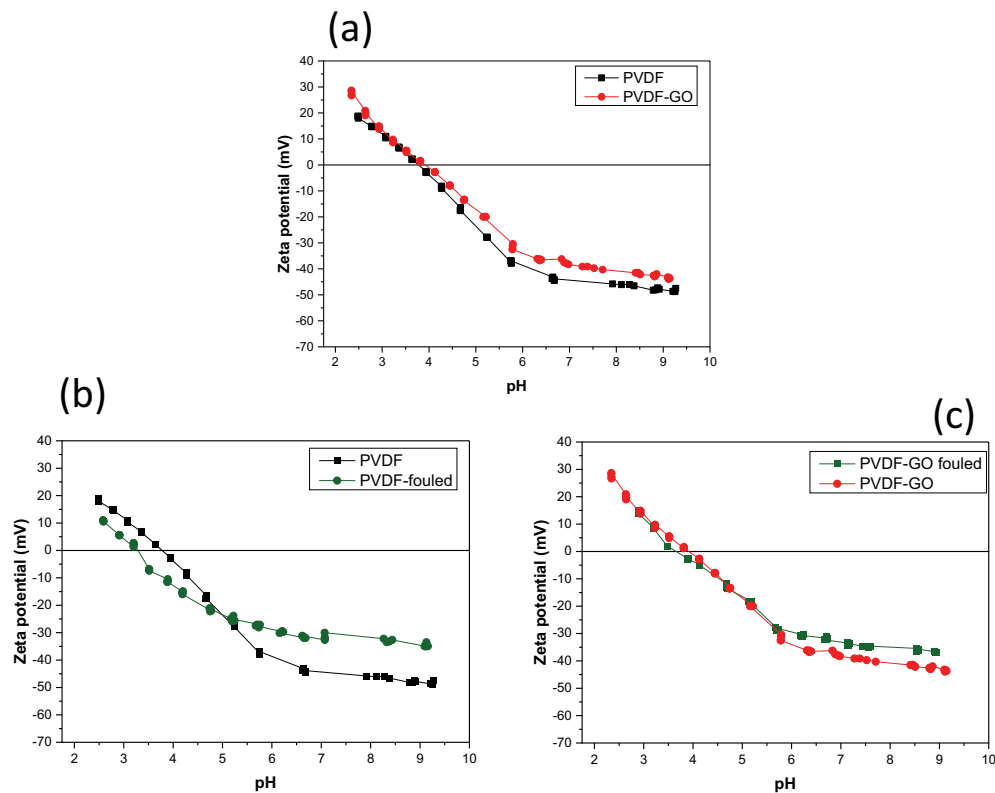
Fig. 6. Zeta potential vs. pH of the pristine (a) and fouled polymeric (b) and mixed matrix (c) membrane.

the GO. The presence of this 2D-nanofiller at low content (1 wt.% with respect to the polymer), was able to modify the structure of the PVDF membranes increasing the dimension of the crystallites, with positive effects on membrane performance, particularly in terms of antifouling properties. The flux and rejection of the mixed matrix membranes were in fact substantially maintained after prolonged contact with humic acids at elevated concentrations, without relevant organic matter deposition on the membrane surface. On the contrary, polymeric PVDF membrane (without GO) was characterized under the same operative conditions by elevated absorption of humid acids on the membrane surface, with consequent severe permeate flux decline in membrane distillation applications (−64% for the PVDF membrane vs. −10% for the PVDF-GO membrane). The results obtained represent a further step head toward the development of membranes specifically designed for MD application.

References

[1] S.M. Fakhrul Islam, Z. Karim, World's Demand for Food and Water: The Consequences of Climate Change, Intechopen, London (UK), 2019.

[2] M.R. Qtaishat, F. Banat, Desalination by solar powered membrane distillation systems, Desalination, 308 (2013) 186–197.

[3] A. Kullab, A. Martin, Membrane distillation and applications for water purification in thermal cogeneration plants, Sep. Purif. Technol., 76 (2011) 231–237.

[4] A. Deshmukh, C. Boo, V. Karanikola, S. Lin, A.P. Straub, T. Tong, D.M. Warsinger, M. Elimelech, Membrane distillation at the water-energy nexus: limits, opportunities, and challenges, Energy Environ. Sci., 11 (2018) 1177–1196.

[5] E. Curcio, G. Di Profio, E. Drioli, Membrane Distillation and Osmotic Distillation, E. Drioli, L. Giorno, Eds., Comprehensive Membrane Science and Engineering, Elsevier B.V, Amsterdam, The Netherlands, 2010, Vol. 4, pp. 1–20.

[6] V. Faggian, P. Scanferla, S. Paulussen, S. Zuin, Combining the European chemicals regulation and an (eco)toxicological screening for a safer membrane development, J. Cleaner Prod., 83 (2014) 404–412.

[7] C. Meringolo, T.F. Mastropietro, T. Poerio, E. Fontananova, G. De Filpo, E. Curcio, G. Di Profio, Tailoring PVDF membranes surface topography and hydrophobicity by a sustainable two-steps phase separation process, ACS Sustainable Chem. Eng., 6 (2018) 10069–10077.

[8] W. Xie, T. Li, A. Tiraferri, E. Drioli, A. Figoli, J.C. Crittenden, B. Liu, Toward the next generation of sustainable membranes from green chemistry principles, ACS Sustainable Chem. Eng., 9 (2021) 50–75.

[9] E.M.V. Hoek, M.T.M. Pendergast, A.K. Ghosh, Nanotechnology-Based Membranes for Water Purification, in: Nanotechnology Applications for Clean Water (2nd ed.), Elsevier, Amsterdam, 2014, pp. 133–154.

[10] R.R. Nair, H.A. Wu, P.N. Jayaram, I.V. Grigorieva, A.K. Geim, Unimpeded permeation of water through helium-leak-tight graphene-based membranes, Science, 335 (2012) 442–444.

[11] S. Dervin, D.D. Dionysiou, S.C. Pillai, 2D nanostructures for water purification: graphene and beyond, Nanoscale, 8 (2016) 15115–15131.

[12] Q. Yang, Y. Su, C. Chi, C.T. Cherian, K. Huang, V.G. Kravets, F.C. Wang, J.C. Zhang, A. Pratt, A.N. Grigorenko, A.K. Geim, R.R. Nair, Ultrathin graphene-based membrane with precise molecular sieving and ultrafast solvent permeation, Nat. Mater., 16 (2017) 1198–1202.

[13] J. Abraham, K.S. Vasu, C.D. Williams, K. Gopinadhan, Y. Su, C.T. Cherian, J. Dix, E. Prestat, S.J. Haigh, I.V. Grigorieva, A.K. Geim, R.R. Nair, Tunable sieving of ions using graphene oxide membranes, Nat. Nanotechnol., 12 (2017) 546–550.

[14] X.-L. Xu, F.-W. Lin, Y. Du, X. Zhang, J. Wu, Z.-K. Xu, Graphene oxide nanofiltration membranes stabilized by cationic porphyrin for high salt rejection, ACS Appl. Mater. Interfaces, 8 (2016) 12588–12593.

[15] C. Zhao, X. Xu, J. Chen, F. Yang, Effect of graphene oxide concentration on the morphologies and antifouling properties of PVDF ultrafiltration membranes, J. Environ. Chem. Eng., 1 (2013) 349–354.

[16] B. Fryczkowska, M. Sieredozka, E. Sarne, R. Fryczkowski, J. Janicki, Influence of a graphene oxide additive and the conditions of membrane formation on the morphology and separative properties of poly(vinylidene fluoride) membranes, J. Appl. Polym. Sci., 132 (2015), doi: 10.1002/APP.42789.

[17] W. Jang, J. Yun, K. Jeonb, H. Byun, PVDF/graphene oxide hybrid membranes via electrospinning for water treatment applications, RSC Adv., 5 (2015) 46711–46717.

[18] R. Gregorio, M. Cestari, Effect of crystallization temperature on the crystalline phase content and morphology of poly(vinylidene fluoride), J. Polym. Sci., Part B: Polym. Phys., 32 (1994) 859–864.

[19] P. Martins, A.C. Lopes, S. Lanceros-Mendez, Electroactive phases of poly(vinylidene fluoride): determination, processing and applications, Prog. Polym. Sci., 39 (2014) 683–706.

[20] S. Majidi Salehi, G. Di Profio, E. Fontananova, F. Nicoletta, E. Curcio, G. De Filpo, Membrane distillation by novel hydrogel composite membranes, J. Membr. Sci., 504 (2016) 220–229.

[21] C. Meringolo, T. Poerio, E. Fontananova, T.F. Mastropietro, F.P. Nicoletta, G. De Filpo, E. Curcio, G. Di Profio, Exploiting fluoropolymers immiscibility to tune surface properties and mass transfer in blend membranes for membrane contactor applications, ACS Appl. Polym. Mater., 1 (2019) 326–334.

[22] E. Fontananova, M.A. Bahattab, S.A. Aljlil, M. Alowairdy, G. Rinaldi, D. Vuono, J.B. Nagy, E. Drioli, G. Di Profio, From hydrophobic to hydrophilic polyvinylidenefluoride (PVDF) membranes by gaining new insight into material's properties, RSC Adv., 5 (2015) 56219–56231.

[23] E. Fontananova, J.C. Jansen, A. Cristiano, E. Curcio, E. Drioli, Effect of additives in the casting solution on the formation of PVDF membranes, Desalination, 192 (2006) 190–197.

[24] G. Naidu, S. Jeong, S. Vigneswaran, Interaction of humic substances on fouling in membrane distillation for seawater desalination, Chem. Eng. J., 262 (2015) 946–957.

[25] D. Jermann, W. Pronk, S. Meylan, M. Boller, Interplay of different NOM fouling mechanisms during ultrafiltration for drinking water production, Water Res., 41 (2007) 1713–1722.

[26] A.H.A. Dehwah, S. Al-Mashharawi, N. Kammourie, T.M. Missimer, Impact of well intake systems on bacterial, algae, and organic carbon reduction in SWRO desalination systems, SAWACO, Jeddah, Saudi Arabia, Desal. Water Treat., 55 (2014) 2594–2600.

[27] A. de la Rubia, M. Rodriguez, D. Prats, pH, Ionic strength and flow velocity effects on the NOM filtration with TiO_2/ZrO_2 membranes, Sep. Purif. Technol., 52 (2006) 325–331.

[28] A. Baglieri, D. Vindrola, M. Gennari, M. Negre, Chemical and spectroscopic characterization of insoluble and soluble humic acid fractions at different pH value, Chem. Biol. Technol. Agric., 1 (2014) 1–11.